



# Heavy metal removal from aqueous solutions by calcium silicate powder from waste coal fly-ash

Jing Ma<sup>a</sup>, Guotong Qin<sup>a,\*</sup>, Yupei Zhang<sup>a</sup>, Junmin Sun<sup>b,\*\*</sup>, Shuli Wang<sup>a</sup>, Lei Jiang<sup>c</sup>

<sup>a</sup> School of Space and Environment, Beihang University, 37 Xueyuan Road, Beijing, 100191, China

<sup>b</sup> National Energy Key Laboratory on Development and Utilization of High Alumina Coal Resources, Hohhot, 010050, China

<sup>c</sup> School of Chemistry, Key Laboratory of Bio-Inspired Smart Interfacial Science and Technology of Ministry of Education, Beihang University, 37 Xueyuan Road, Beijing, 100191, China

## ARTICLE INFO

### Article history:

Available online 13 February 2018

### Keywords:

Calcium silicate powder  
Adsorption  
Heavy metal  
Mechanism

## ABSTRACT

The removal of Ni (II), Cu (II), Zn (II), and Co (II) ions from simulated aqueous solutions using calcium silicate powder (CSP), a new by-product derived from the production of alumina from coal ash, has been studied. CSP showed high efficiency for the removal of these metal ions. The maximum adsorptions were 420.17, 680.93, 251.89, and 235.29 mg/g for Ni (II), Cu (II), Zn (II), and Co (II), respectively. Total (100%) removal of Ni (II) was obtained when the initial concentration was 100 mg/L, indicating that CSP was highly effective even at an extremely low concentration. Adsorption isotherms and kinetics have been studied using different models. It has been found that the adsorption isotherms can best be described on the basis of the Langmuir model, with the kinetics of adsorption following a pseudo-second-order reaction process. The calcium ion concentration was examined before and after adsorption to investigate the mechanism of removal of the heavy metal ions. It was found that the removal of heavy metal ions is mainly achieved through ion-exchange, combined with some adsorption.

© 2018 Elsevier Ltd. All rights reserved.

## 1. Introduction

Heavy metal pollution has become an increasingly serious environmental problem in recent decades, causing numerous diseases and disorders. An action plan for tackling soil pollution in China was released on 28th May 2017. The Action Plan for Soil Pollution Prevention and Control aims to improve soil quality, ensure safe agricultural products and a healthy living environment for people, according to the State Council, China's cabinet. To control soil pollution by heavy metals, China has vowed to cut the discharge of major heavy metal pollutants in key industries by 10% by 2020. Finding a highly efficient remediation technology remains a bottleneck. Various processes exist for removing dissolved heavy metals from aqueous solutions, including ion-exchange, precipitation, phytoextraction, ultrafiltration, reverse osmosis, electrocoagulation, electro dialysis, and adsorption. Adsorption, particularly using low-cost adsorbents, has attracted a great deal of attention from the research community and industry due to its high

efficiency and simplicity of operation.

Numerous studies have been reported regarding the adsorption of heavy metals by both natural and artificial adsorbents. Natural zeolites, which are abundant, low-cost adsorbents, show high adsorption capacity for heavy metal ions in water (Erdem et al., 2004). The kinetics (Kocaoba et al., 2007; Motsi et al., 2011; Panayotova and Velikov, 2002), equilibrium (Kocaoba et al., 2007), and influence of temperature and pH (Jimenez et al., 2004) have been investigated in relation to these materials. Activated carbon adsorbents are widely used in the removal of heavy metals (Adebisi et al., 2017; Demiral and Güngör, 2016; Jusoh et al., 2007; Kang et al., 2008; Tounsadi et al., 2016). Carbon nanotubes and graphene, as new carbon adsorbents, have also been applied in the removal of heavy metals (Duru et al., 2016; Gu et al., 2015; Gupta et al., 2016; Ihsanullah et al., 2016; Sahraei et al., 2017). Biosorption is an alternative for the removal of heavy metals due to its low cost and eco-friendly nature (Alluri et al., 2007; Basu et al., 2017; Mudhoo et al., 2012; Tang et al., 2017; Wang and Chen, 2009). Reducing the cost of adsorbents is a critical issue for spreading the use of adsorption technologies for the removal of heavy metals.

Synthesized calcium silicates as low cost adsorbents have been used in removing heavy metals. Tobermorites were made from

\* Corresponding author.

\*\* Corresponding author.

E-mail addresses: [qingt@buaa.edu.cn](mailto:qingt@buaa.edu.cn) (G. Qin), [sunjmdt@163.com](mailto:sunjmdt@163.com) (J. Sun).

waste container glass using hydrothermal method and showed high removal capacities for  $\text{Cd}^{2+}$  and  $\text{Zn}^{2+}$  (Coleman et al., 2006, 2014). Functionalized calcium silicate nanofibers were derived from oyster shells for removal of heavy metal ions, showing removal capacity of 203 and  $256 \text{ mg g}^{-1}$  for  $\text{Cu(II)}$  and  $\text{Cr(VI)}$  cations (You et al., 2016). The cement based materials have been widely researched for stabilization or solidification of heavy metals (Chen et al., 2009; Tommaseo and Kersten, 2002). All these studies showed the potential application of calcium silicates in the removal of heavy metals.

Coal remains one of the main energy resources. Indeed, coal accounted for 62.0% of the total energy consumption in China in 2016 (Statistical Communiqué of the People's Republic of China on the 2016 National Economic and Social Development [http://www.stats.gov.cn/english/PressRelease/201702/t20170228\\_1467503.html](http://www.stats.gov.cn/english/PressRelease/201702/t20170228_1467503.html)). Fly-ash is one of the emission pollutants of coal combustion, with about 60 million tonnes being discharged annually in China. Dust and soluble components of fly-ash present great risks to the environment. Comprehensive utilization of fly-ash is considered of great importance by the Chinese government. Fly-ash is mainly composed of alumina and silica, with some other metal oxides. Coal resources with aluminum contents in the coal ash of over 50% are abundant in the northwest of China. Overall, the reserve of this kind of ash in China exceeds 20 billion tonnes. A demo-refinery for coal-ash-based alumina has been constructed in the Inner Mongolia Autonomous Region. The strategy of producing alumina from fly-ash has been a typical case of cyclic economy in China. This alumina production route was released as a Chinese policy in 2013. The fly-ash represents an alternative raw material for alumina due to the shortage of bauxite in China. However, the silica-based by-product constitutes a secondary pollutant and will influence the economic efficiency of the production of alumina from fly-ash if it cannot be effectively reused. Therefore, exploring novel routes for the utilization of this silica-based by-product is a promising strategy. During alumina refining, the silica in the fly-ash is removed as calcium silicate powder (CSP), a new by-product. Employment of CSP as an adsorbent to remove heavy metals in water, thereby controlling pollution with waste, should achieve a win-win situation for the economy and the environment.

Herein, we report the mechanism of  $\text{Ni}^{2+}$ ,  $\text{Cu}^{2+}$ ,  $\text{Zn}^{2+}$ , and  $\text{Co}^{2+}$  removal by CSP from alumina production, along with data on its performance, to pave a way for application of CSP. It has been found that the high adsorption capacity of CSP for heavy metal ions results from ion-exchange. The CSP has shown super removal capacities of the four used heavy metals. The environmental benefit for soil pollution control has been analyzed.

## 2. Experimental method

### 2.1. Chemicals and materials

CSP was supplied by Inner Mongolia Datang International Renewable Energy Resource Development Co., Ltd. (Hohhot, China) and was used as received. Nickel (II) nitrate and cobalt (II) chloride were purchased from Tianjin JINKE Fine Chemical Research Institute (Tianjin, China). Ammonium citrate, dimethylglyoxime, ethylenediamine tetraacetic acid tetrasodium salt, hydroxylamine hydrochloride, copper (II) sulfate, zinc(II) nitrate, and sodium pyrophosphate were purchased from Xilong Scientific (Guangdong, China). Sulfuric acid, sodium citrate, acetic acid, orthoboric acid, sodium hydroxide, and hydrochloric acid were purchased from Beijing Chemicals (Beijing, China). 2,9-Dimethyl-1,10-phenanthroline, zincon monosodium salt, 4-(5-chloro-2-pyridylazo)-1,3-diaminobenzene, ethylenediaminetetraacetic acid

(EDTA), and 2-hydroxy-1-(2-hydroxy-4-sulfo-1-naphthylazo)-3-naphthoic acid were purchased from Sinopharm Chemical Reagent Beijing Co., Ltd. (Beijing, China). All reagents were of analytical grade and were used without further purification.

### 2.2. Adsorption

Solutions containing  $\text{Ni}^{2+}$ ,  $\text{Cu}^{2+}$ ,  $\text{Zn}^{2+}$ , and  $\text{Co}^{2+}$  were prepared by dissolving nickel (II) nitrate, copper (II) sulfate, zinc(II) nitrate, and cobalt (II) chloride, respectively, in deionized water. Simulated wastewaters containing different concentrations of these four ions were prepared to test the adsorption capacities of CSP. The initial concentrations of  $\text{Ni}^{2+}$  and  $\text{Cu}^{2+}$  are 200, 400, 600, 800, 900 and 1000 mg/L respectively. The initial concentrations of  $\text{Zn}^{2+}$  are 200, 400, 600, 800 and 1000 mg/L. The initial concentrations of  $\text{Co}^{2+}$  are 100, 200, 300, 400, 500, 600, and 700 mg/L.

Metal uptake experiments were performed in batch reactors (250 mL flasks) placed in a shaker bath. Each metal ion adsorption tests were conducted using six flasks, each containing 0.1 g of CSP and 100 mL of solution. At predetermined time intervals, the adsorption process in one of the flasks was stopped and the solution was filtered to analyze the metal ion concentration. Each flask was used only once, retrieving data for just one time interval to avoid possible errors deriving from changes in the ratio between adsorbent material and solution caused by the removal of the sample solution for analysis. The  $\text{Ni}^{2+}$ ,  $\text{Cu}^{2+}$ ,  $\text{Zn}^{2+}$ , and  $\text{Co}^{2+}$  contents were analyzed by spectrophotometry using dimethylglyoxime (National Standard of the People's Republic of China, GB/T 11910–1989, Water quality-Determination of nickel- Dimethylglyoxime spectrophotometric method), 2,9-dimethyl-1,10-phenanthroline (National Environmental Protection Standard of the People's Republic of China, HJ 486-2009, Water quality-Determination of copper-2,9-dimethyl-1,10-phenanthroline spectrophotometric method), zincon monosodium salt (National Standard of the People's Republic of China, GB/T 10656–2008, Analysis of water used in boiler and cooling-Determination of Zinc-Zincon Spectrophotometry), and 4-(5-chloro-2-pyridylazo)-1,3-diaminobenzene (National Environmental Protection Standard of the People's Republic of China, HJ 550-2015, Water quality-Determination of cobalt-5-Cl-PADAB Spectrophotometry), respectively. The  $\text{Ca}^{2+}$  concentration was analyzed through the EDTA titrimetric method (National Standard of the People's Republic of China, GB 7476–87, Water quality-Determination of calcium- EDTA titrimetric method).

The adsorption of metal ions by CSP was calculated according to:

$$R(\%) = \frac{C_0 - C_e}{C_0} \times 100 \quad (1)$$

where  $R$  is the removal of metal ions and  $C_0$  and  $C_e$  are the initial and equilibrium concentrations (mg/L), respectively.

$$R(\%) = \frac{C_0 - C_e}{C_0} \times 100 \quad (2)$$

where  $q_e$  is the equilibrium adsorption capacity,  $V$  is the volume of the metal ion solution (L), and  $W$  is the weight of the adsorbent (g).

Several models have been proposed in the literature to describe adsorption isotherms. In this study, the Langmuir and Freundlich isotherm models were used to describe the relationship between metal ion adsorption and the equilibrium concentration in solution.

The Langmuir model assumes monolayer adsorption and that the surface of adsorbents consists of identical adsorption sites. The linear form of the Langmuir isotherm is expressed as (Huang et al., 2012):

$$\frac{C_e}{q_e} = \frac{1}{q_{\max} K_L} + \frac{C_e}{q_{\max}} \quad (3)$$

where  $q_e$  (mg/g) is the amount of metal ion adsorbed per unit mass of adsorbent,  $C_e$  (mg/L) is the equilibrium concentration of the metal ion, and  $q_{\max}$  (mg/g) and  $K_L$  (L/mg) are the Langmuir constants related to the adsorption capacity and adsorption rate, respectively.

The Freundlich model assumes that the surface of the adsorbent is heterogeneous and that stronger binding sites are occupied first. The model is described by the equation:

$$\log q_e = \log K_F + \frac{1}{n} \log C_e \quad (4)$$

where  $K_F$  is a characteristic parameter of the adsorption capacity ( $[\text{mg/g}]/[\text{mg/L}]^{1/n}$ ), and  $n$  is the adsorption intensity.

Pseudo-first-order and pseudo-second-order models (Schiewer and Patil, 2008) were used in this work to describe the rate of metal ion uptake on the CSP.

$$\text{First - order model : } \log(q_e - q_t) = \log q_e - \frac{k_t t}{2.303} \quad (5)$$

$$\text{Second - order model : } \frac{t}{q_t} = \frac{1}{k_2 q_e^2} + \frac{t}{q_e} \quad (6)$$

### 2.3. Characterization

The crystal structure of the CSP was studied by X-ray diffraction (XRD; D/max2200 PC, Rigaku, Japan) using  $\text{Cu-K}\alpha$  radiation, over the  $2\theta$  range from  $10^\circ$  to  $80^\circ$ . The surface area of the CSP was determined through nitrogen adsorption at 77 K on an ASAP 2020 instrument (Micromeritics, Norcross, GA, USA). The chemical composition of the CSP was determined by X-ray fluorescence spectrometry (XRF; S4-Explorer, Bruker Corporation, Karlsruhe, Germany). The particle size distribution of the CSP was measured by the laser scattering technique (Mastersizer, 2000, Malvern Instruments Ltd., Malvern, UK).

## 3. Adsorption of heavy metals

### 3.1. Analysis of the CSP

The composition of the CSP is shown in Table 1. It was mainly composed of  $\text{SiO}_2$  and  $\text{CaO}$ , with small amounts of impurities. The particle size was about  $17 \mu\text{m}$  (Fig. 1) and the crystalline phase was mainly calcium silicate hydroxide (Riversideite-9A) (shown in Fig. 2). The surface area of the CSP was  $50.68 \text{ m}^2/\text{g}$ .

### 3.2. Adsorption isotherms

Fig. 3 shows the adsorption isotherms of the CSP for metal ions. The equilibrium adsorption increased with increasing concentration of the heavy metal ions. It should be noted that the amounts of  $\text{Ni}^{2+}$ ,  $\text{Cu}^{2+}$ ,  $\text{Zn}^{2+}$ , and  $\text{Co}^{2+}$  adsorbed at equilibrium were 387.2,

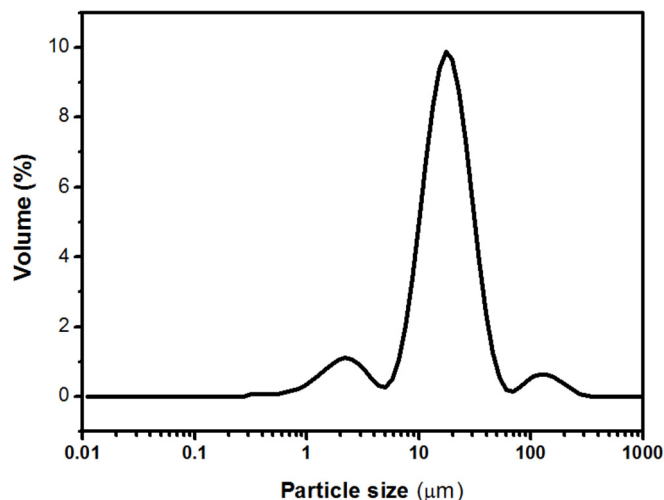


Fig. 1. Particle size distribution of CSP.

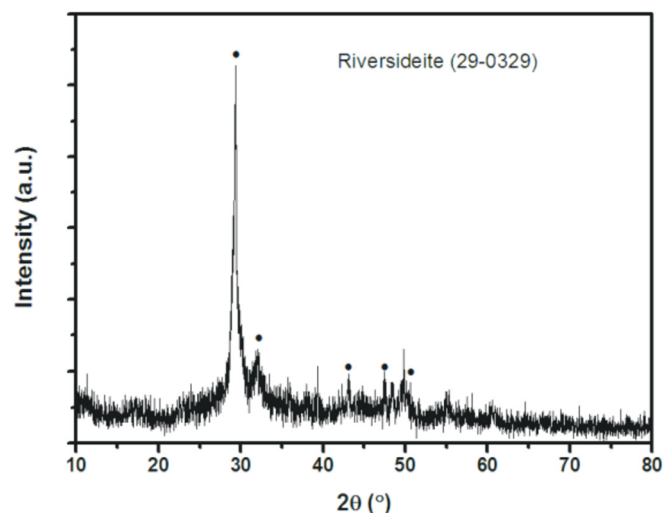


Fig. 2. XRD profile of CSP.

399.89, 197.68, and 195.81 mg/g when the equilibrium concentrations were as low as 12.80, 0.11, 1.16, and 4.19 mg/L, respectively. This indicates that these four metal ions can be effectively removed even at low equilibrium concentrations. Furthermore,  $\text{Ni}^{2+}$  was no longer detected when the solution was analyzed after adsorption (initial concentration of  $\text{Ni}^{2+}$  200 mg/L), showing its complete removal by the CSP, even at extremely low concentrations.

Fig. 4 shows the linear relationships of  $C_e/q_e$  versus  $C_e$  and of  $\log q_e$  versus  $\log C_e$ . Table 2 shows the parameters of the Langmuir and Freundlich models. The Langmuir model accurately described the adsorption of the four metal ions by CSP; the  $R^2$  correlation values were all  $>0.999$  for these relationships. The maximum adsorptions ( $q_{\max}$ ) were 420.17, 680.93, 251.89, and 235.29 mg/g for  $\text{Ni}^{2+}$ ,  $\text{Cu}^{2+}$ ,  $\text{Zn}^{2+}$ , and  $\text{Co}^{2+}$ , respectively. The adsorption capacities were very high compared to the results achieved with carbon nanotubes

**Table 1**  
Composition of the CSP (wt%).

$\text{Na}_2\text{O}$	$\text{MgO}$	$\text{Al}_2\text{O}_3$	$\text{SiO}_2$	$\text{P}_2\text{O}_5$	$\text{SO}_3$	Cl	$\text{K}_2\text{O}$	$\text{CaO}$	$\text{TiO}_2$	$\text{Fe}_2\text{O}_3$	SrO
3.77	0.592	1.03	42.7	0.191	0.271	0.0975	0.0509	50.9	0.0940	0.130	0.0234

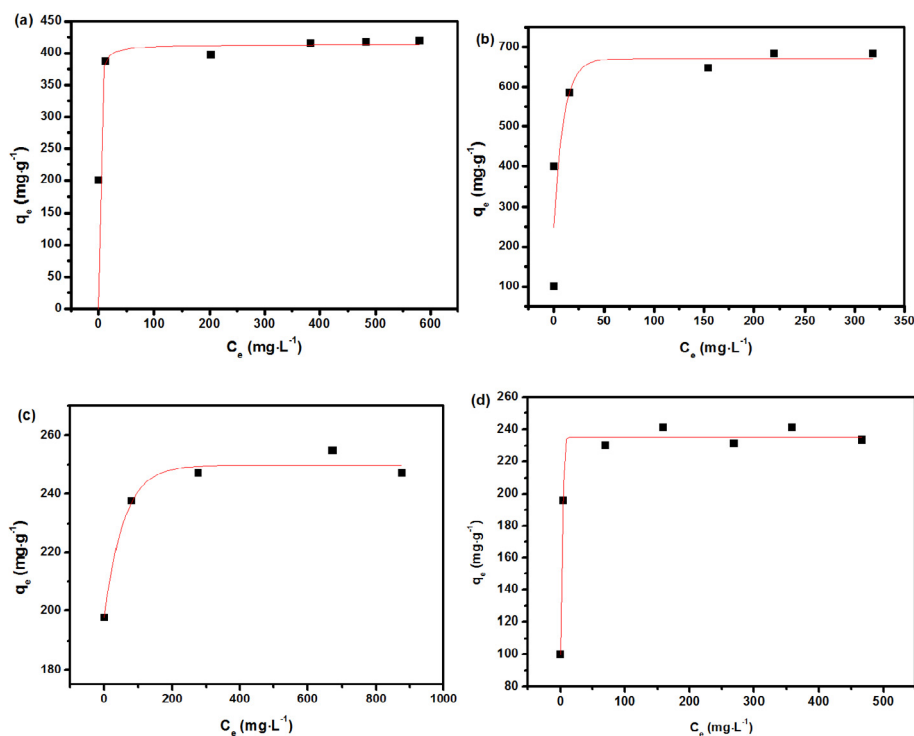


Fig. 3. Adsorption isotherms of CSP for metal ions: (a) nickel (II), (b) copper (II), (c) zinc(II), and (d) cobalt (II).

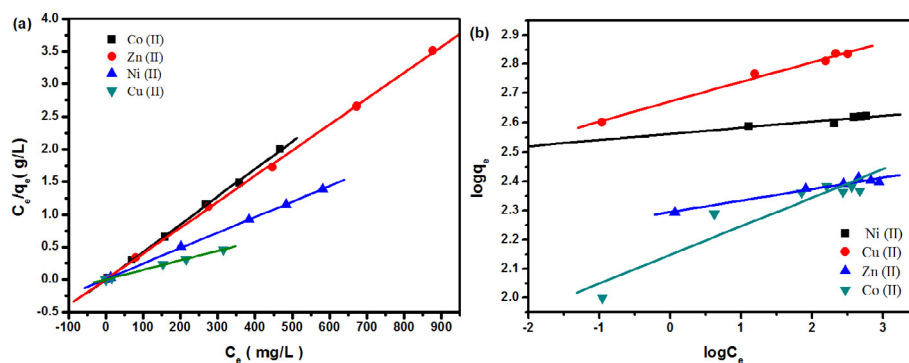


Fig. 4. Langmuir (a) and Freundlich (b) adsorption isotherms of metal ions onto CSP.

Table 2

Characteristic parameters and coefficients of the experimental data according to the Langmuir and Freundlich models.

Ion	Langmuir isotherms				Freundlich isotherms		
	$R^2$	$q_{\max}$ (mg/g)	$K_L$ (L/mg)	$R_L$	$R^2$	$1/n$	$K_F$ (l/mg) $\times 10^{-2}$
$\text{Ni}^{2+}$	0.9998	420.17	0.3005	0.0033	0.9733	0.0205	3.6543
$\text{Cu}^{2+}$	0.9996	680.93	0.5029	0.0020	0.9869	0.0677	4.6938
$\text{Zn}^{2+}$	0.9997	251.89	1.1711	0.00008	0.9743	0.0396	1.9706
$\text{Co}^{2+}$	0.9996	235.29	70.8333	0.00002	0.8717	0.0982	1.4051

(Gupta et al., 2016), carbon foams (Lee et al., 2016), biochar (Inyang et al., 2016), alga (Kuyucak and Volesky, 1989), natural zeolites (Erdem et al., 2004), or ion-exchange resins (Kang et al., 2004). The Langmuir model gave  $R^2$  correlation coefficients  $>0.99$ , fitting the experimental data better than the Freundlich isotherm.

### 3.3. Adsorption kinetics of $\text{Ni}^{2+}$ , $\text{Cu}^{2+}$ , $\text{Zn}^{2+}$ , and $\text{Co}^{2+}$ onto CSP

The adsorption of metal ions onto CSP versus time is shown in

Fig. 5. The initial concentration of the metal ions was 400 mg/L.  $\text{Cu}^{2+}$  ion showed the highest adsorption rate and it was no longer detected in the solution after 1 h of adsorption. The estimated removals of  $\text{Ni}^{2+}$ ,  $\text{Co}^{2+}$ , and  $\text{Zn}^{2+}$  were 96.98%, 60.75%, and 30.47%, respectively.

Fig. 6 shows the relationship of  $\log(q_e - q_t)$  versus  $t$  and plots of the values of  $t/q_t$  against  $t$  for the adsorption of the metal ions onto CSP. The parameters  $k_1$ ,  $k_2$ , and  $q_e$ , determined from the slopes and intercepts of the curves, are shown in Table 3. There are notable

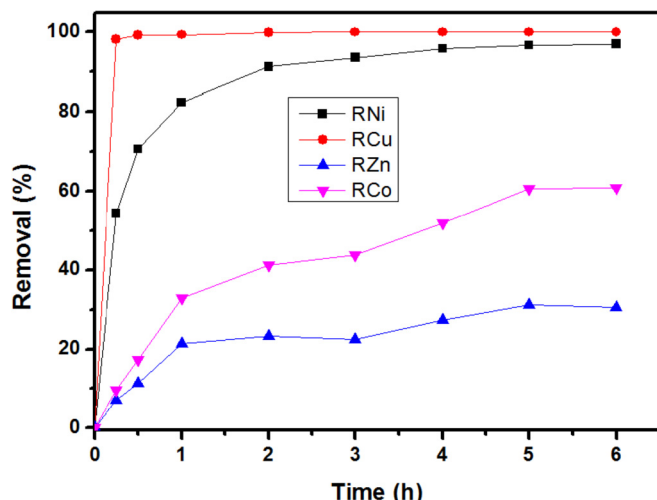


Fig. 5. Kinetic adsorption curves of CSP for heavy metals (the initial metal ion concentration was 400 mg/L).

differences between the experimental and theoretical values, indicating that the first-order model does not fit the data well over the entire range of contact times studied. On the other hand, the pseudo-second-order model fits the experimental data quite well.

### 3.4. Mechanism of the adsorption of metal ions on the CSP

In spite of the high adsorption of metal ions, since the surface area of the CSP was only 50.68 m<sup>2</sup>/g, it is not reasonable that the uptake of metal ions was due to adsorption alone. Moreover, it was found that the process could best be described by a second-order reaction. It is well known that silicates often show considerable ion-exchange ability. To gain more insight into the mechanism of metal ion removal, the calcium ion concentration was determined before and after adsorption. The results are shown in Table 4. The sample indicated as “Blank” was a control sample containing only

CSP. The equilibrium concentration of calcium was 26.42 mg/L, indicating that the CSP had been partially dissolved. For the four test solutions, complete removal of the heavy metal ions was achieved, with final concentrations of 0 mg/L in the equilibrated solutions. On the other hand, the calcium ion concentration increased considerably compared to the blank sample, indicating that ion-exchange had occurred. The increase in calcium ion concentration was nevertheless lower than the amount of absorbed heavy metal ions, suggesting that their removal does not occur uniquely through an ion-exchange process. Considering that the surface area of the CSP was 50.68 m<sup>2</sup>/g, it is reasonable that adsorption also contributed to the removal of the heavy metal ions.

## 4. Environmental and economic benefits

The application of CSP in the removal of heavy metals from water will clean the water, collect heavy metals, and reduce soil pollution. We chose Inner Mongolia Datang International Recycling Resource Development (IMDIRRD) Co., Ltd. (Hohhot, China) as a case to evaluate the environmental and economic benefit of CSP adsorption as a means of removing heavy metals. IMDIRRD was founded in 2007 for the re-utilization of coal fly-ash from a coal-fired power plant. The main product of IMDIRRD is alumina produced from coal fly-ash. A demo-line has been constructed, with a production of alumina of 200,000 tonnes per annum, along with 150,000 tonnes of CSP. This route for the utilization of coal fly-ash has been one of the typical cases of cyclic economics in China. If all of the 150,000 tonnes of CSP could be used as an adsorbent to remove heavy metals from water, the benefits will not only be water cleaning, but also the recovery of heavy metals and reducing soil pollution.

Based on the previous experimental results, the adsorption capacity of CSP for heavy metals increased with the equilibrium concentrations. To ensure that the treated water would meet environmental requirements, the adsorption capacities were selected as 200, 400, 100, and 100 mg/g for Ni<sup>2+</sup>, Cu<sup>2+</sup>, Co<sup>2+</sup>, and Zn<sup>2+</sup> respectively. It should be noted that such adsorption capacities would be worthwhile for the recovery of heavy metals. The

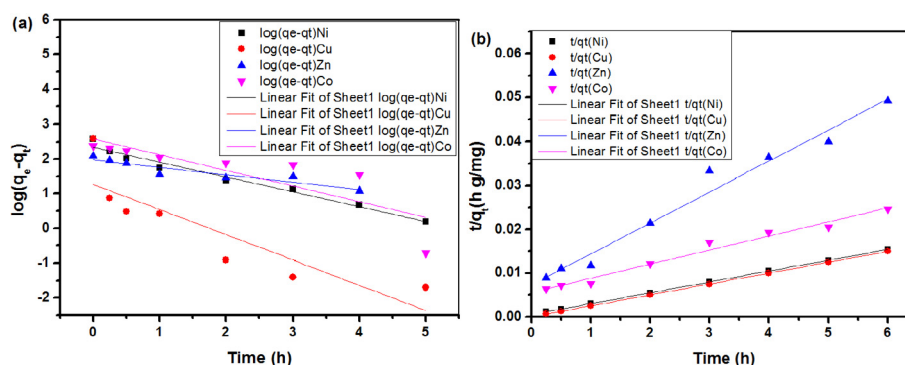


Fig. 6. Pseudo-first-order (a) and pseudo-second-order (b) kinetics for adsorption of metal ions onto CSP.

Table 3

Comparison of the pseudo-first-order and pseudo-second-order adsorption rate constants for the adsorption of metal ions onto CSP.

Ion	$Q_{e,exp}$ (mg/g)	Pseudo-first-order model			Pseudo-second-order model		
		$Q_{e,cal}$ (mg/g)	$K_1$ (h <sup>-1</sup> )	$R^2$	$Q_{e,cal}$ (mg/g)	$K_2$ (g/(mg·h))	$R^2$
Ni <sup>2+</sup>	387.92	220.21	0.9809	0.9702	401.61	0.0117	0.9999
Cu <sup>2+</sup>	399.89	18.66	1.6747	0.7141	400.00	0.5364	1
Zn <sup>2+</sup>	121.87	95.68	0.4972	0.8484	141.84	0.0068	0.9730
Co <sup>2+</sup>	243.02	384.55	1.0451	0.6453	309.60	0.0019	0.9764



**Table 4**

Calcium ion concentrations before and after adsorption.

Samples	Initial			Equilibrium		
	C <sub>heavy metal</sub> (mg/L)	C <sub>Ca2+</sub> (mg/L)	heavy metal ion (mmol)	C <sub>heavy metal</sub> (mg/L)	C <sub>Ca2+</sub> mg/L	calcium ion (mmol)
Blank	0	0	0	0	26.42	0.0659
Ni <sup>2+</sup>	100	0	0.1704	0	67.05	0.1673
Cu <sup>2+</sup>	100	0	0.1574	0	60.34	0.1501
Zn <sup>2+</sup>	100	0	0.1530	0	60.26	0.1503
Co <sup>2+</sup>	100	0	0.1697	0	66.65	0.1663

**Table 5**

Economic and environmental benefits of application of CSP in the treatment of heavy-metal-polluted water.

Heavy metal	Adsorption capacity, mg/g	Heavy metal concentration in waste water, mg/L	Recovery of heavy metal, tonnes	Cleaning water, 10 <sup>6</sup> tonnes	Reduction of polluted soil, hectare
Ni <sup>2+</sup>	200	50–100	3000	300–600	53,571–107,143
Cu <sup>2+</sup>	400	50–100	6000	600–1200	107,143–214,286
Zn <sup>2+</sup>	100	50–100	1500	150–300	26,786–53,571
Co <sup>2+</sup>	100	50–100	1500	150–300	26,786–53,571

heavy metal concentration in the waste water was selected as 50–100 mg/L, a general range for industrial waste water containing heavy metals. When treating water containing heavy metals at this concentration, the heavy metals can be collected almost completely. The reduction of soil pollution was calculated based on the assumption that the water will be used for irrigation in the North China Plain Region. The total amount of all the irrigations was selected as 80 mm, while full irrigation was considered as four irrigations for wheat and three irrigations for maize (Sun et al., 2015; Xiao et al., 2017). Therefore, the amount of water for irrigation was 5600 m<sup>3</sup>/hectare. Table 5 shows the analysis results concerning the potential benefit of application of CSP in the removal of heavy metals from waste water. If all the CSP from the demo-line at IMDIRRD were to be used as an adsorbent for the removal of heavy metals from water, the benefits will cover water cleaning, recovery of heavy metals, and reduction of soil pollution. Based on the above selected conditions, the amount of heavy metals recovered will be 1500–6000 tonnes, and the treated water and reduction of polluted soil will be 1.50–12 × 10<sup>8</sup> tonnes and 26,786–214,286 ha respectively.

## 5. Conclusions

CSP is a new kind of by-product from the procedure for the production of alumina from solid waste coal fly-ash. CSP has been investigated as an adsorbent for the removal of Ni<sup>2+</sup>, Cu<sup>2+</sup>, Zn<sup>2+</sup>, and Co<sup>2+</sup> ions from simulated solutions. A high adsorption capacity of these heavy metals onto CSP was achieved, with maximum adsorptions in the range of hundreds of mg/g. The isotherms were well described by the Langmuir model. Kinetic studies have indicated that the adsorption of heavy metals follows a pseudo-second-order equation, indicating chemisorption. The mechanism of the removal of heavy metals by CSP has been delineated. The change in calcium cation concentration shows that the removal of heavy metals is to a great extent due to an ion-exchange process. Re-utilization of CSP as a low cost adsorbent for removal heavy metal in water not only offers an application of this by-product, but also offers great environmental and economic benefits. CSP can be used to clean waste water containing heavy metal and recycle the heavy metals.

## Acknowledgement

The authors are thankful for the financial support by the

National Key Technology R&D Program of China (2009BAB49B02).

## References

- Adebisi, G.A., Chowdhury, Z.Z., Alaba, P.A., 2017. Equilibrium, kinetic, and thermodynamic studies of lead ion and zinc ion adsorption from aqueous solution onto activated carbon prepared from palm oil mill effluent. *J. Clean. Prod.* 148, 958–968.
- Alluri, H.K., Ronda, S.R., Settalluri, V.S., Singh, J., Bondili, S.V., Venkateshwar, P., 2007. Biosorption: an eco-friendly alternative for heavy metal removal. *Afr. J. Biotechnol.* 6, 2924–2931.
- Basu, M., Guha, A.K., Ray, L., 2017. Adsorption of lead on cucumber peel. *J. Clean. Prod.* 151, 603–615.
- Chen, Q.Y., Tyrer, M., Hills, C.D., Yang, X.M., Carey, P., 2009. Immobilisation of heavy metal in cement-based solidification/stabilisation: a review. *Waste Manag.* 29, 390–403.
- Coleman, N.J., Brassington, D.S., Raza, A., Lee, W.E., 2006. Calcium silicate sorbent from secondary waste ash: heavy metals-removal from acidic solutions. *Environ. Technol.* 27, 1089.
- Coleman, N.J., Li, Q., Raza, A., 2014. Synthesis, structure and performance of calcium silicate ion exchangers from recycled container glass. *Physicochem. Problem. Miner. Process.* 50, 5–16.
- Demiral, H., Güngör, C., 2016. Adsorption of copper(II) from aqueous solutions on activated carbon prepared from grape bagasse. *J. Clean. Prod.* 124, 103–113.
- Duru, I., Ege, D., Kamali, A.R., 2016. Graphene oxides for removal of heavy and precious metals from wastewater. *J. Mater. Sci.* 51, 6097–6116.
- Erdem, E., Karapinar, N., Donat, R., 2004. The removal of heavy metal cations by natural zeolites. *J. Colloid Interface Sci.* 280, 309–314.
- Gu, X.Y., Yang, Y., Hu, Y., Wang, C.Y., 2015. Fabrication of graphene-based xerogels for removal of heavy metal ions and capacitive deionization. *ACS Sustain. Chem. Eng.* 3, 1056–1065.
- Gupta, V.K., Moradi, O., Tyagi, I., Agarwal, S., Sadegh, H., Shahryari-Ghosheh, R., Makhlof, A.S.H., Goodarzi, M., Garshasbi, A., 2016. Study on the removal of heavy metal ions from industry waste by carbon nanotubes: effect of the surface modification: a review. *Crit. Rev. Environ. Sci. Technol.* 46, 93–118.
- Huang, J., Jin, X., Deng, S., 2012. Phenol adsorption on an N-methylacetamide-modified hypercrosslinked resin from aqueous solutions. *Chem. Eng. J.* 192, 192–200.
- Ihsanullah, Abbas A., Al-Amer, A.M., Laoui, T., Al-Marri, M.J., Nasser, M.S., Khraisheh, M., Atieh, M.A., 2016. Heavy metal removal from aqueous solution by advanced carbon nanotubes: critical review of adsorption applications. *Separ. Purif. Technol.* 157, 141–161.
- Inyang, M.I., Gao, B., Yao, Y., Xue, Y.W., Zimmerman, A., Mosa, A., Pullammanappallil, P., Ok, Y.S., Cao, X.D., 2016. A review of biochar as a low-cost adsorbent for aqueous heavy metal removal. *Crit. Rev. Environ. Sci. Technol.* 46, 406–433.
- Jimenez, R.S., Dal Bosco, S.M., Carvalho, W.A., 2004. Heavy metals removal from wastewater by the natural zeolite scolecite - temperature and pH influence in single-metal solutions. *Quim. Nova* 27, 734–738.
- Jusoh, A., Shiung, L.S., Ali, N.A., Noor, M.J.M.M., 2007. A simulation study of the removal efficiency of granular activated carbon on cadmium and lead. *Desalination* 206, 9–16.
- Kang, K.C., Kim, S.S., Choi, J.W., Kwon, S.H., 2008. Sorption of Cu<sup>2+</sup> and Cd<sup>2+</sup> onto acid- and base-pretreated granular activated carbon and activated carbon fiber samples. *J. Ind. Eng. Chem.* 14, 131–135.
- Kang, S.-Y., Lee, J.-U., Moon, S.-H., Kim, K.-W., 2004. Competitive adsorption

- characteristics of  $\text{Co}^{2+}$ ,  $\text{Ni}^{2+}$ , and  $\text{Cr}^{3+}$  by IRN-77 cation exchange resin in synthesized wastewater. *Chemosphere* 56, 141–147.
- Kocaoba, S., Orhan, Y., Akyuz, T., 2007. Kinetics and equilibrium studies of heavy metal ions removal by use of natural zeolite. *Desalination* 214, 1–10.
- Kuyucak, N., Volesky, B., 1989. Accumulation of cobalt by marine alga. *Biotechnol. Bioeng.* 33, 809–814.
- Lee, C.G., Song, M.K., Ryu, J.C., Park, C., Choi, J.W., Lee, S.H., 2016. Application of carbon foam for heavy metal removal from industrial plating wastewater and toxicity evaluation of the adsorbent. *Chemosphere* 153, 1–9.
- Motsi, T., Rowson, N.A., Simmons, M.J.H., 2011. Kinetic studies of the removal of heavy metals from acid mine drainage by natural zeolite. *Int. J. Miner. Process.* 101, 42–49.
- Mudhoo, A., Garg, V.K., Wang, S.B., 2012. Removal of heavy metals by biosorption. *Environ. Chem. Lett.* 10, 109–117.
- Panayotova, M., Velikov, B., 2002. Kinetics of heavy metal ions removal by use of natural zeolite. *J. Environ. Sci. Health Part A Toxic Hazard. Subst. Environ. Eng.* 37, 139–147.
- Sahraei, R., Sekhavat Pour, Z., Ghaemy, M., 2017. Novel magnetic bio-sorbent hydrogel beads based on modified gum tragacanth/graphene oxide: removal of heavy metals and dyes from water. *J. Clean. Prod.* 142 (Part 4), 2973–2984.
- Schiewer, S., Patil, S.B., 2008. Pectin-rich fruit wastes as biosorbents for heavy metal removal: equilibrium and kinetics. *Bioresour. Technol.* 99, 1896–1903.
- Sun, H., Zhang, X., Wang, E., Chen, S., Shao, L., 2015. Quantifying the impact of irrigation on groundwater reserve and crop production – a case study in the North China Plain. *Eur. J. Agron.* 70, 48–56.
- Tang, J., Li, Y., Wang, X., Daroch, M., 2017. Effective adsorption of aqueous  $\text{Pb}^{2+}$  by dried biomass of *Landoltia punctata* and *Spirodela polyrrhiza*. *J. Clean. Prod.* 145, 25–34.
- Tommaseo, C.E., Kersten, M., 2002. Aqueous solubility diagrams for cementitious waste stabilization systems. 3. Mechanism of zinc immobilization by calcium silicate hydrate. *Environ. Sci. Technol.* 36, 2919–2925.
- Tounsadi, H., Khalidi, A., Abdenouni, M., Barka, N., 2016. Activated carbon from *Diplotaxis Harra* biomass: optimization of preparation conditions and heavy metal removal. *J. Taiwan Inst. Chem. Eng.* 59, 348–358.
- Wang, J.L., Chen, C., 2009. Biosorbents for heavy metals removal and their future. *Biotechnol. Adv.* 27, 195–226.
- Xiao, D., Shen, Y., Qi, Y., Moiwo, J.P., Min, L., Zhang, Y., Guo, Y., Pei, H., 2017. Impact of alternative cropping systems on groundwater use and grain yields in the North China Plain Region. *Agric. Syst.* 153, 109–117.
- You, W.J., Hong, M.Z., Zhang, H.F., Wu, Q.P., Zhuang, Z.Y., Yu, Y., 2016. Functionalized calcium silicate nanofibers with hierarchical structure derived from oyster shells and their application in heavy metal ions removal. *Phys. Chem. Chem. Phys.* 18, 15564–15573.